Summer research: fall of magnet through a conducting tube

Martin Okanik

October 28, 2020

Abstract

This work discusses the dynamics of a dipole magnet falling through a thin cylindrical conducting tube. Formulae for magnetic fields, forces, torque and induced voltages are derived for a magnet free to move translationally in the plane of symmetry of the problem, and to rotate around axis perpendicular to this plane. These expressions are also found analytically in terms of elliptic integrals. Simulations were performed to study the trajectory. This is a work in progress, and so there is more left to do to check and complete the simulation code. Future plan is to study the dynamics of a superconductive setup.

1 Introduction

Fall of bar magnet through a metallic pipe is a simple demonstration of Lenz's and Faraday's laws. It is commonly seen on public outreach events, where the audience can be puzzled by unexpectedly long travel time of a small bar magnet through a narrow tube (as narrow as possible, due to strong influence of braking force on radius, as we shall see). The induced magnetic currents are creating magnetic field which produces a repulsive force on the bar magnet. Equivalently, the mechanical energy of the falling body is transfered to electromagnetic energy and dissipated as RI^2 thermal losses. Donoso et al have studied [1] the case of magnet falling on-axis, having also experimentally verified their calculations. In their later papers [2],[3] they included more interesting cases such as a magnet falling off the axis of symmetry or two magnets falling together. In their work, they neglected the rotation of the magnet. This is not unreasonable, as for most real life settings, (all) moments of inertia of a magnet with usual magnetization values are too high for significant rotation to be seen, at least on the timescale of its fall through a regular conductive pipe.

However, investigating the dynamics of such a coupled electromagnetic system is not only mildly interesting on its own, but also useful in far more intriguing problems. In particular, the behaviour of a magnet above/inside a superconducting tube. It was predicted theoretically by Levin and Rizzato [4] that a

magnet should fall freely once inside the tube. To get there, a considerable energy barrier must be overcome. As a result, many magnets will simply levitate above the tube, as suggests our general intuition of Meissner's effect. This prediction was experimentally verified in 2012 by Welsh and Severn [5] and was found to be incorrect. Instead, the magnet is trapped anywhere in the tube, with any orientation. It does not fall for the duration of the superconducting state and can be moved at will. Rotation is quickly damped by eddy currents. These features were also observed more recently by Williams et al. [6] in their educational experiment.
The ultimate goal of this research is to build a robust numerical model of the superconductive system, try to recover the experimental behaviour and explain it theoretically. To get there, we first decided to study the standard conducting case and set up a reliable finite difference scheme for solving all the dynamics of this system. This was further subdivided into progressively more complex models , each of which was built on the previous one. The most complex and general case that we considered so far was a freely rotating magnet moving in $x-z$ plane, and free to rotate in this plane. This means that no initial azimuthal impulse was given (i.e. perpendicular to the $x-z$ plane, which remains the plane of symmetry of this problem). These calculations are presented one by one in next section and the corresponding simulation results are presented in separate chapter.

2 Methods

2.1 General remarks and on-axis fall of parallel magnet

2.1.1 Calculations for a conductive ring

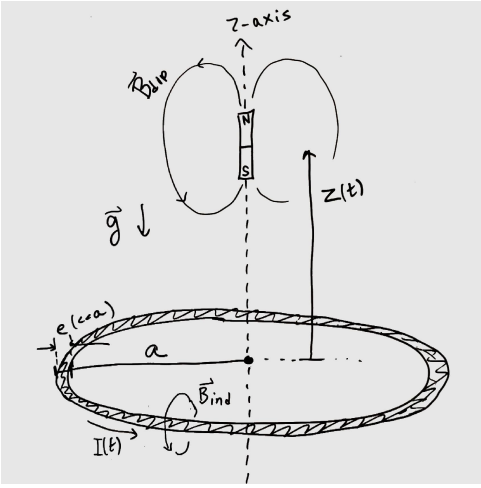

Figure 1: Magnet falling centrally through a thin ring

To study a problem like a magnet falling through a conductive tube, one needs to choose a suitable partitioning of the tube. A "thin tube" is such that its thickness is much smaller than its radius ($e << a$). In this case, let us divide the tube into N rings along z-axis, so for a tube of height H, the height of one ring is $dz = H/N$. Resistance of such elemental ring is then $R = \frac{2\pi a}{\sigma e dz}$ One obtains N ohmic equations of form $RI_i = \epsilon_i, i \in [1, N]$, where ϵ is the induced e.m.f. for the given ring. The e.m.f. has two contributions: there is variable magnetic flux from the falling magnetic dipole field and a contribution from the variations of all other currents in the tube. For a centered magnet parallel to z-axis, one obtains the system:

$$M\ddot{z} = -Mg + F_{mag}(z, I) \tag{1}$$

$$R\dot{I} = \epsilon_{mag}(z, \dot{z}) + \epsilon_{tube}(\dot{I}) \tag{2}$$

This system of ODEs should be treated numerically, after obtaining the functional dependence of forces and voltages. This can be done either (i) analytically, or (ii) numerically. Analytical solution is simple for a centered and parallel magnet and a conductive ring in $x - y$ plane:

$$F_{mag,z} = \frac{3\mu_0 m a^2}{2} \frac{z(t)I(t)}{(a^2 + z(t)^2)^{3/2}} \tag{3}$$

$$\epsilon_{mag} = \frac{3\mu_0 m a^2}{2} \frac{z(t)\dot{z}(t)}{(a^2 + z(t)^2)^{3/2}} \tag{4}$$

where the dipole moment is $\boldsymbol{m} = (0, 0, m)$. Magnetic force is calculated from the formula $\boldsymbol{F_{mag}} = (\boldsymbol{m} \cdot \nabla)\boldsymbol{B} = m_z \partial_z B_z \boldsymbol{e_z}$ for a dipole field $\frac{\mu_0}{4\pi} \frac{3\hat{\boldsymbol{r}}(\boldsymbol{m}\cdot\hat{\boldsymbol{r}}) - \boldsymbol{m}}{|\boldsymbol{r}|^3}$. Flux cutting (hence ϵ_{mag} from this moving field can either be obtained as surface integral $-\partial_t \int_S \boldsymbol{B} \cdot \boldsymbol{dS}$ or as line integral $\oint_{\partial S} (\boldsymbol{v} \times \boldsymbol{B}) \cdot \boldsymbol{dl}$.

2.1.2 Terminal velocity in a tube

For the case of a long, thin tube, we can derive an easy expression for the terminal speed. Neglecting the self-inductance and calling the symmetry of the problem:

$$\epsilon = RI = \frac{2\pi a}{e\sigma dz} I = -2\pi a \dot{z} B_\rho(\rho, z) \tag{5}$$

where B_ρ is the radial component of the magnetic field, which can be found e.g. by Biot-Savart law to be:

$$B_\rho(\rho = a, z) = \frac{\mu_0}{4\pi} \frac{3mza}{(a^2 + z^2)^{5/2}} \tag{6}$$

Combining these expressions with that for magnetic force, we arrive at:

$$F_{mag,z} = -\frac{9}{8\pi} \mu_0^2 a e \sigma m^2 a^2 \dot{z} \int_{tube} \frac{z^2}{(a^2 + z^2)^5} dz \tag{7}$$

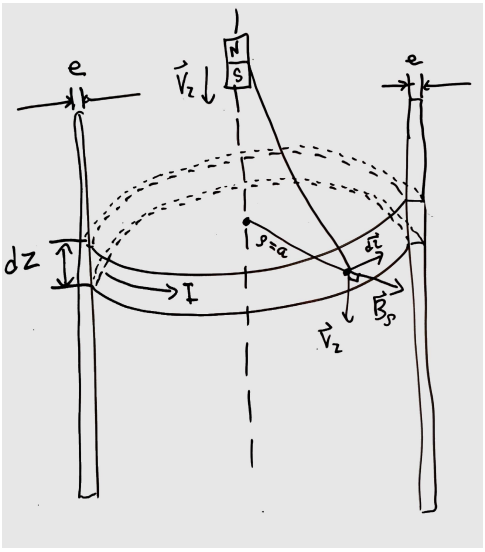

Figure 2: Illustration of induced voltage for a ring forming a (long) tube

We see that integrand decays as $1/z^3$ for $z >> a$, so for a long tube, contributions from elemental rings many radii away from magnet are negligible. Define $v = \frac{z}{a}$. We can then formally replace this integral over finite region by that over the entire v-axis:

$$F_{mag,z} = -\frac{9\mu_0^2 e\sigma m^2}{8\pi a^4}\dot{z}\int_{-\infty}^{+\infty}\frac{v^2}{(1+v^2)^5}dv \tag{8}$$

The definite integral above evaluates to $\frac{5\pi}{128}$ and hence:

$$F_{mag,z} = -\frac{45\mu_0^2 e\sigma m^2}{1024a^4}\dot{z} = -K\dot{z} \tag{9}$$

This can then be inserted into 2nd Newton's Law to get $M\ddot{z} + K\dot{z} + Mg = 0$, hence the terminal speed:

$$v_t = \frac{1024a^4 Mg}{45\mu_0^2 e\sigma m^2} \tag{10}$$

2.1.3 Self-inductance

Calculating the self inductance of the tube relies on summing contributions from fluxes of rings of currents with different mutual distances. Consider flux linked by ring C due to current I' in ring C', both rings being displaced by z:

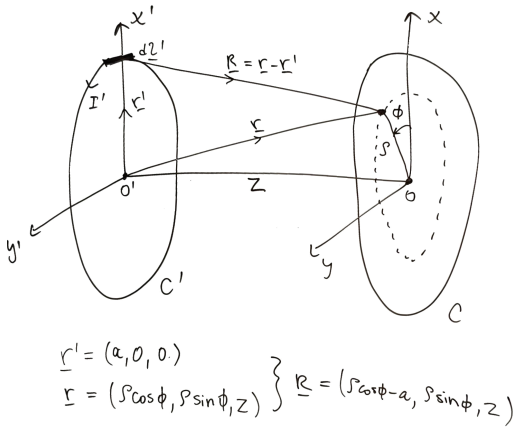

Figure 3: Derivation of mutual inductance of two thin rings of radius a spaced z apart

$$d^3\Phi = d\boldsymbol{B}\cdot\boldsymbol{dS} = \frac{\mu_0 I'}{4\pi R^3}\left(\begin{pmatrix}0\\ad\phi'\\0\end{pmatrix}\times\begin{pmatrix}\rho\cos\phi - a\\ \rho\sin\phi\\ z\end{pmatrix}\right)\cdot\begin{pmatrix}0\\0\\ \rho d\phi d\rho\end{pmatrix} \tag{11}$$

Integrating through ϕ' yields simply 2π and hence we get:

$$M(z) = \frac{\Phi}{I'} = \int_{\phi=0}^{2\pi}\int_{\rho=0}^{a}\frac{\mu_0\rho(a-\rho\cos\phi)d\rho d\phi}{2(\rho^2+a^2+z^2-2a\rho\cos\phi)^{3/2}} \tag{12}$$

One only needs to do this once, before the simulation starts - distances between rings making up the tube do not change during the simulation. Otherwise, this calculation would introduce a quadratic dependence of computation cost on the number of partitions.

Note: in numerical calculations, role of self-induced e.m.f. $\epsilon_{tube}(\dot{I})$ was neglected as a second order effect, but this approximation needs more careful analysis! File "tube_off_axis_withTubeInductance.ipynb" (Python) and "finite_thin(ish)_tube_onaxis.nb" (Mathematica) are developing self-inductance calculations, but they do not (yet) work (reliably).

2.2 Off-axis calculations

As one moves off-axis, symmetry in the geometry of our problem is broken. Without loss of generality, label the direction of initial displacement of magnet

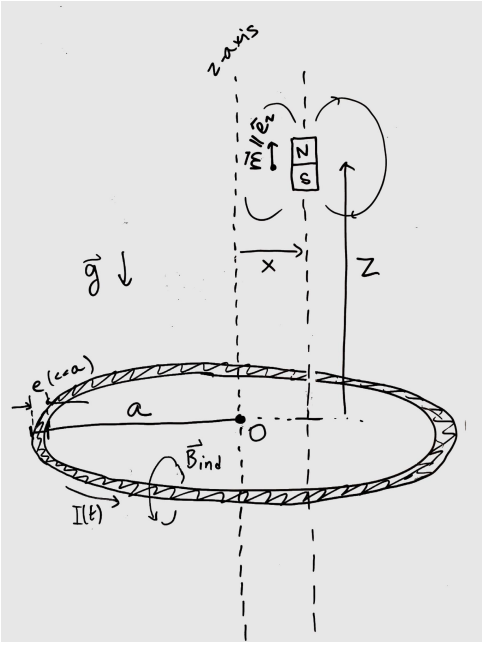

Figure 4: Magnet falling through a thin ring, with displacement $x(t)$ from axis of cylindrical symmetry

as the x-axis. Magnet keeps moving in $x-z$ plane, as long as it is not given initial velocity along y-axis, which does not happen (...as we assume). For now, assume that magnetic dipole moment remains parallel to z-axis. This can correspond e.g. to a magnet with high moment of inertia (at least compared to its magnetisation). The formula for magnetic force now gives

$$\boldsymbol{F_{mag}} = (\boldsymbol{m}\cdot\nabla)\boldsymbol{B} = m_z\partial_z B_z \boldsymbol{e_z} + m_z \partial_z B_x \boldsymbol{e_x} \tag{13}$$

Starting again from Biot-Savart law, we can derive formulae for both components of the B-field. Let $u = x/a$ and $v = z/a$ be dimensionless spatial coordinates, suitable for the purposes of integration. z is understood here as the relative coordinate of magnet w.r.t. ring.

$$B_x^{ring} = \frac{\mu_0 I}{4\pi a}\int_0^{2\pi} \frac{v\cos\phi}{(1+u^2+v^2-2uv\cos\phi)^{3/2}}d\phi \tag{14}$$

$$B_z^{ring} = \frac{\mu_0 I}{4\pi a}\int_0^{2\pi} \frac{1-u\cos\phi}{(1+u^2+v^2-2uv\cos\phi)^{3/2}}d\phi \tag{15}$$

It can be seen that first expression integrates to zero as $u \to 0$ and it can be shown that second integral reduces to standard formula for on-axis field of a loop of current. After taking relevant spatial derivatives, we get expressions for

the components of magnetic force:

$$F_x^{ring} = m_z \frac{\mu_0 I}{4\pi a^2} \int_0^{2\pi} \cos\phi \frac{1 + u^2 - 2v^2 - 2u\cos\phi}{(1 + u^2 + v^2 - 2uv\cos\phi)^{5/2}} d\phi \tag{16}$$

$$F_z^{ring} = -m_z \frac{3\mu_0 I}{4\pi a^2} \int_0^{2\pi} \frac{1 - u\cos\phi}{(1 + u^2 + v^2 - 2uv\cos\phi)^{5/2}} d\phi \tag{17}$$

We still need to find the expression for $\epsilon_{mag}(z, \dot{z})$. It is more efficient (computationally) to calculate it as a line integral $\oint_{\partial S} (\boldsymbol{v} \times \boldsymbol{B}) \cdot \boldsymbol{dl}$ rather than the surface integral $-\partial_t \int_S \boldsymbol{B} \cdot \boldsymbol{dS}$.

Take a velocity vector $(\dot{x}, 0, \dot{z})$ and dipole magnetic field $\frac{\mu_0}{4\pi} \frac{3\hat{\boldsymbol{r}}(\boldsymbol{m}\cdot\hat{\boldsymbol{r}}) - \boldsymbol{m}}{|\boldsymbol{r}|^3}$ with $\boldsymbol{m} = (0, 0, m)$. One arrives at the following intermediate formula for the induced voltage:

$$\epsilon_{mag} = \frac{\mu_0 m}{4\pi a} \int_0^{2\pi} \frac{\left(\dot{x}\cos\phi\left(a^2 - 2ax\cos\phi + x^2 - 2z^2\right) - 3z\dot{z}(a - x\cos\phi)\right)}{\left(a^2 - 2ax\cos\phi + x^2 + z^2\right)^{5/2}} d\phi \tag{18}$$

A reasonable approximation would be to ignore the terms in $\dot{x}$, as the radial velocity is expected to be much smaller than vertical velocity at all points in time (including the terminal velocities). This assumption can be checked retrospectively. After once again, making the integral dimensionless, one gets:

$$\epsilon_{mag} \approx \frac{3\mu_0 m\dot{z}}{4\pi a^2} \int_0^{2\pi} \frac{v(1 - u\cos\phi)}{\left(1 - 2u\cos\phi + u^2 + v^2\right)^{5/2}} d\phi \tag{19}$$

We previously (i.e. on the axis of symmetry) used Wolfram Mathematica's *NDSolve*, the built-in function for numerical solution of systems of ODEs. However, this strategy is trickier to use for off-axis case, when there are no simple expressions for F_{mag} and ϵ_{mag}. *NDSolve* is unable to solve the system when the sought functions $(x(t), z(t), I(t))$ and their derivatives appear inside other functions for numerical integration. There are 2 possible ways round this issue:

1. seek analytical expressions for the integrals above to insert into *NDSolve* and solve the system of ODEs as before

2. change algorhitm into explicit finite difference method, storing all values in arrays and updating time manually, so that one has access to instantaneous values of physical quantities on each iteration - hence can use them in numerical routines at will

For the first approach, Mathematica's powerful symbolic computation capabilities were of great help. We derived closed analytical expressions for ϵ_{mag} and both components of $\boldsymbol{F_{mag}}$ in terms of elliptic integrals. These expressions are too long and are given in Appendix.
Second approach consisted of re-writing all the simulations in Python and use the *NumPy* and *SciPy* modules for efficient computations with large matrices.

2.3 Fall with rotation

Let us now add third degree of freedom (DoF) α - angle of rotation around y-axis. This new DoF has a simple equation of motion (EoM) which takes form:

$$\ddot{\alpha} = \frac{G_y}{\mathcal{I}_{yy}} = \frac{m_z B_x - m_x B_z}{\mathcal{I}_{yy}} = \frac{m(B_x \cos\alpha - B_z \sin\alpha)}{\mathcal{I}_{yy}} \tag{20}$$

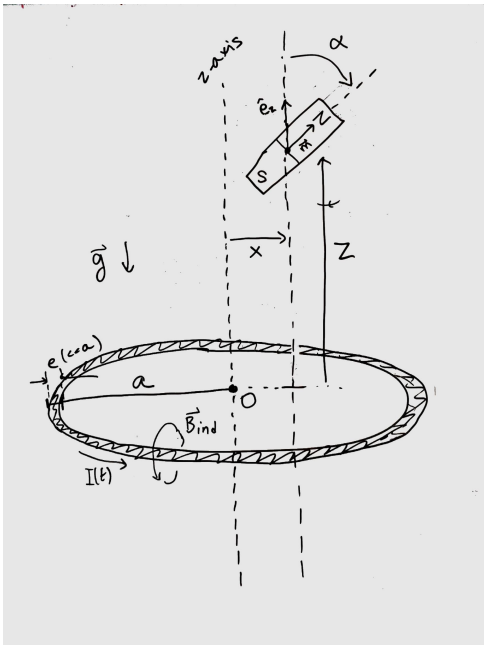

Figure 5: Magnet falling through a thin ring, free to rotate in $x-z$ plane with angle $\alpha(t)$ from z-axis

The expression for magnetic force is also more complex, as there is now non-zero m_x and hence also spatial derivatives with respect to x:

$$\boldsymbol{F_{mag}} = (\boldsymbol{m}\cdot\nabla)\boldsymbol{B} = (m_z\partial_z B_z + m_x\partial_x B_z)\boldsymbol{e_z} + (m_z\partial_z B_x + m_x\partial_x B_x)\boldsymbol{e_x} \tag{21}$$

We are missing only the derivatives $\partial_x B_x$ and $\partial_x B_z$. Again, derive them for a single ring in $x-y$ plane and magnet at $(x,0,z)$:

$$\partial_x B_x = -\frac{3\mu_0 I}{4\pi a^2}\int_0^{2\pi} \frac{v\cos\phi(u-\cos\phi)}{(1+u^2+v^2-2uv\cos\phi)^{5/2}}d\phi \tag{22}$$

$$\partial_x B_z = \frac{\mu_0 I}{4\pi a^2}\int_0^{2\pi} \frac{-3u+(2+2u^2-v^2)\cos\phi - u\cos^2\phi}{(1+u^2+v^2-2uv\cos\phi)^{5/2}}d\phi \tag{23}$$

We also need to calculate the e.m.f. in the ring. Again, integrate the vector product of velocity with the dipole field $\frac{\mu_0}{4\pi}\frac{3\hat{\boldsymbol{r}}(\boldsymbol{m}\cdot\hat{\boldsymbol{r}})-\boldsymbol{m}}{|\boldsymbol{r}|^3}$ along its circumference.Use

the same approximation for velocity vector as before: $\boldsymbol{v} \approx \dot{z}\boldsymbol{e_z}$:

$$\epsilon_{mag} = \oint_{\partial S} \left(\begin{pmatrix} 0 \\ 0 \\ \dot{z} \end{pmatrix} \times \begin{pmatrix} B_x \\ B_y \\ B_z \end{pmatrix} \right) \cdot a \begin{pmatrix} -\sin\phi \\ \cos\phi \\ 0 \end{pmatrix} d\phi \tag{24}$$

This evaluates to:

$$\epsilon_{mag} = \dot{z} \int_0^{2\pi} (B_y(\phi)\sin\phi + B_x(\phi)\cos\phi) d\phi \tag{25}$$

$B_x(\phi)$ and $B_y(\phi)$ are analytical expressions of variables x, z, a, ϕ and are given below:

2.4 Numerical implementation

For the most general system as described in last section, we have the following set of ODEs:

$$\ddot{x} = \frac{1}{M} F_x(x, z, \alpha, I) \tag{26}$$

$$\ddot{z} = -g + \frac{1}{M} F_z(x, z, \alpha, I) \tag{27}$$

$$\ddot{\alpha} = \frac{1}{\mathcal{I}} G_y(x, z, \alpha, I) \tag{28}$$

$$RI = \epsilon_{mag}(x, z, \dot{z}, \alpha) + \epsilon_{tube}(\dot{I}) \tag{29}$$

We implemented two numerical algorithms to solve this system (example for z-coordinate):

2.4.1 Modified leapfrog algorithm

We used standard leapfrog procedure for calculating the three DoFs for the magnet, here is example of z-coordinate:

$$a_z(i) = -g + f_z(x(i), z(i), \alpha(i), I_n(i)) \tag{30}$$

$$v_z(i + 1/2) = v_z(i - 1/2) + dt \times a_z(i) \tag{31}$$

$$z(i + 1) = z(i) + dt \times v(i + 1/2) \tag{32}$$

I_n is current in n-th ring, we need all N of these, so the relevant data structure is an N-dimensional vector. First iteration must be done manually for this algorithm. $x(0), \dot{x}(0), z(0), \dot{z}(0), \alpha(0), \dot{\alpha}(0), I_n(0)$ are provided by initial conditions, so we obtained derivatives at $i = 1/2$ as e.g.

$$v_z(1/2) = v_z(0) + \frac{dt}{2} \times a_z(0) \tag{33}$$

Currents were calculated as

$$I_n(i+1) = \frac{1}{R}\epsilon_{mag}\left(z(i+1), v_z(i+1/2) + \frac{dt}{2} \times a_z(i), \alpha(i+1)\right) \tag{34}$$

which has drawback that the velocity relevant for calculation of current is known very poorly and essentially cancels the advantage of leapfrog method over the simplest forward Euler algorithm. Different algorhitm should be employed to increase accuracy.

2.4.2 RK4 algorithm

We then implemented the standard fourth-order Runge-Kutta (RK4) algorithm for six variables - all three DoFs and their time derivatives. Additional variables calculated from these are currents I_n for $1 < i < N$, N being the number of partitions of tube. Let us define the notation as follows (example of one-dimensional system):

$$\dot{v}(t) = f(x(t), v(t)) \tag{35}$$
$$\dot{x}(t) = v(t) \tag{36}$$

$$k_{v,1} = f\left(x(t), v(t)\right) dt \tag{37}$$
$$k_{x,1} = v(t)dt \tag{38}$$
$$k_{v,2} = f\left(x(t) + \frac{k_{x,1}}{2}, v(t) + \frac{k_{v,1}}{2}\right) dt \tag{39}$$
$$k_{x,2} = \left(v(t) + \frac{k_{v,1}}{2}\right) dt \tag{40}$$
$$k_{v,3} = f\left(x(t) + \frac{k_{x,2}}{2}, v(t) + \frac{k_{v,2}}{2}\right) dt \tag{41}$$
$$k_{x,3} = \left(v(t) + \frac{k_{v,2}}{2}\right) dt \tag{42}$$
$$k_{v,4} = f\left(x(t) + k_{x,3}, v(t) + k_{v,3}\right) dt \tag{43}$$
$$k_{x,4} = \left(v(t) + k_{v,3}\right) dt \tag{44}$$
$$\tag{45}$$

Then the updated steps are

$$x(t+dt) = x(t) + \frac{1}{6}(k_{x,1} + 2k_{x,2} + 2k_{x,3} + k_{x,4})$$
$$v(t+dt) = v(t) + \frac{1}{6}(k_{v,1} + 2k_{v,2} + 2k_{v,3} + k_{v,4})$$

In our case, the system looks like (e.g. second step for z-coordinate):

$$k_{v_z,2} = \left(-g + f\left(x(i) + \frac{k_{x,1}}{2}, z(i) + \frac{k_{z,1}}{2}, v_z(i) + \frac{k_{v_z,1}}{2}, \alpha(i) + \frac{k_{\alpha,1}}{2}, I_{n;(i,2)}\right)\right) dt \tag{46}$$

where the instantaneous current in n-th tube element for the second RK4 step at iteration i is $I_{n;(i,2)}$, and it is calculated based on relevant values of other quantities:

$$I_{n;(i,2)} = \frac{1}{R}\epsilon_{mag}\left(x(i) + \frac{k_{x,1}}{2}, z(i) + \frac{k_{z,1}}{2}, v_z + \frac{k_{v_z,1}}{2}, \alpha(i) + \frac{k_{\alpha,1}}{2}\right) \tag{47}$$

Hence there is no further complication to calculating current and RK4 is actually easier to implement than original low order algorhitm. This self-starting property would not hold if we also considered the second term: $\epsilon_{tube}(\dot{I}_n)$, as the appearance of time derivative would require knowing future values of every I_n.

3 Results

3.1 On-axis fall

We verified the formula (10) for the terminal velocity of the magnet as function of varying dipole moment and tube radius. The physical parameters were:

- length of tube H: 10 m
- radius of tube a: variable or fixed at 5 cm
- thickness of tube (only to calculate resistance of a ring, tube assumed thin for physical purposes): 1 cm
- conductivity σ: 5.92×10^{-7} $Siemens \times m$ (i.e. that of copper)
- dipole moment m: variable or fixed at 2 A/m^2
- mass of magnet M: 3 g
- g-acceleration: 9.81 m/s^{-2}

The tube was partitioned into $N = 10^4$ rings and the timestep was 2 ms. Simulations yielded very good agreement with the above theoretical result (valid for a thin tube of infinite extent).

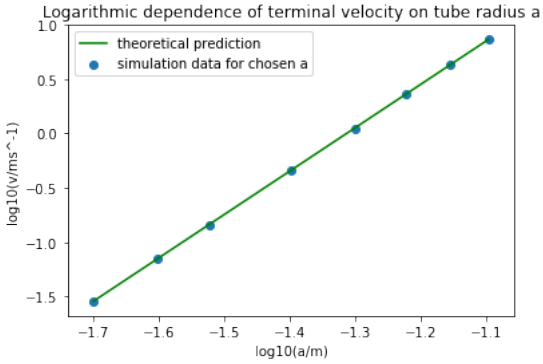

Figure 6: Perfect agreement with the theoretical value was observed for the dependence of velocity on tube radius.

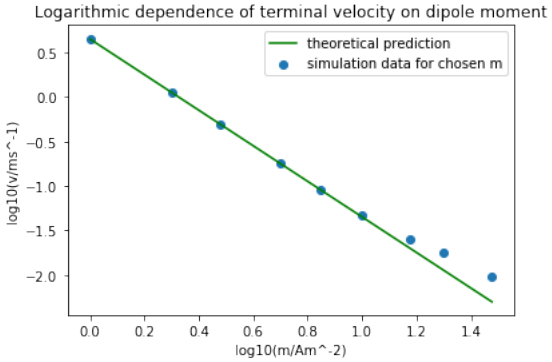

Figure 7: A departure from inverse quadratic trend was observed for large dipole moments, its origins were not yet resolved.

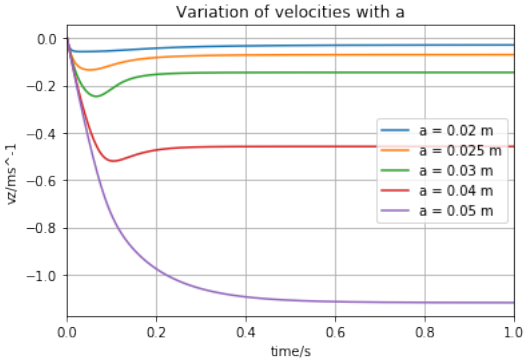

Figure 8: Temporal evolution of velocities for different radii. Note the overshoot due to Lenz's law. It is more prominent (in relative terms) for smaller radii and hence more prominent electromagnetic effects compared to gravity. The transient regime lasts under 0.5 s.

3.2 Off-axis fall without rotation

Parameters were similar as for on-axis case, except that the tube was just 1 m long and partitioned into 200 rings, with timestep set to 1 ms.
The formulae for forces and voltages derived in subsection 2.2 are plotted here:

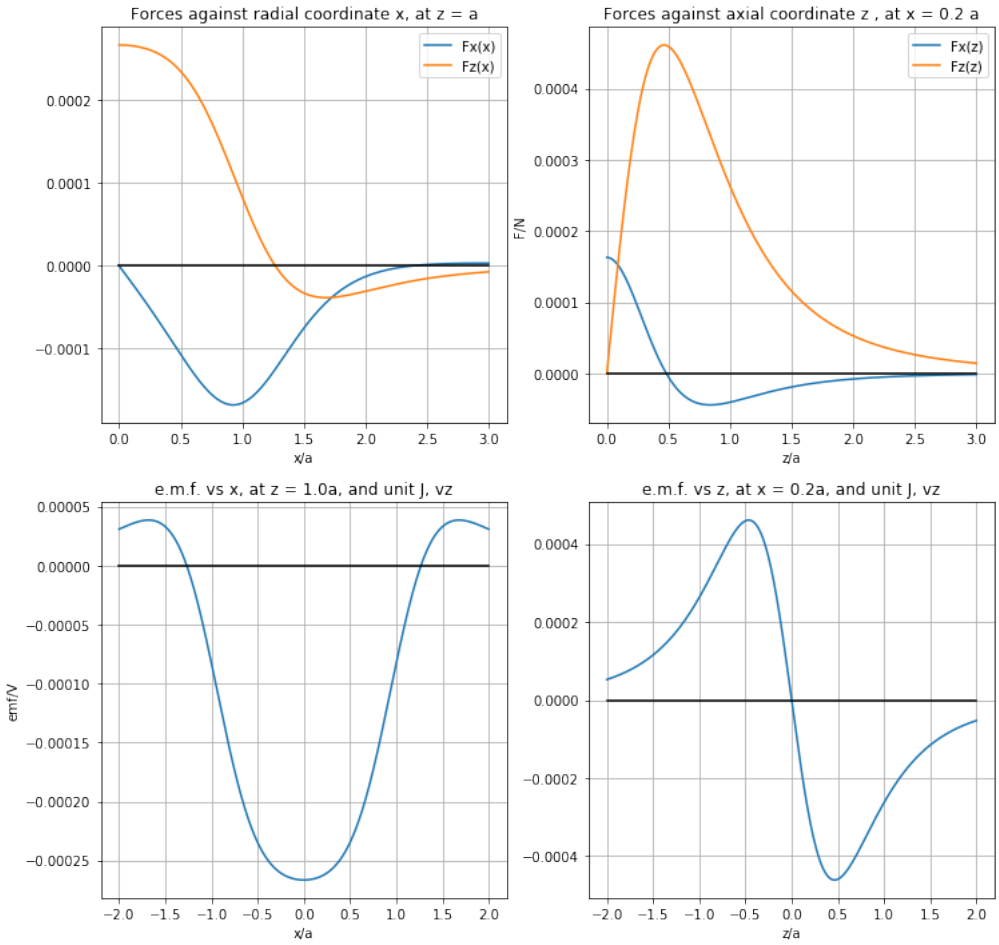

Figure 9: Forces in both directions and ϵ_{mag} ploted against both axes. "a" denotes the radius of the tube. The absolute scale of forces is decided by a choice of physical parameters and is not important in this example. Radial force $F_x(x)$ is attractive and approximately linear near axis, so we would expect simple harmonic motion to be possible for small displacements. HOWEVER, it seems that it becomes repulsive for rings that are very close in z-direction (top right graph). This behaviour was not expected, but no error was discovered in the derivations.

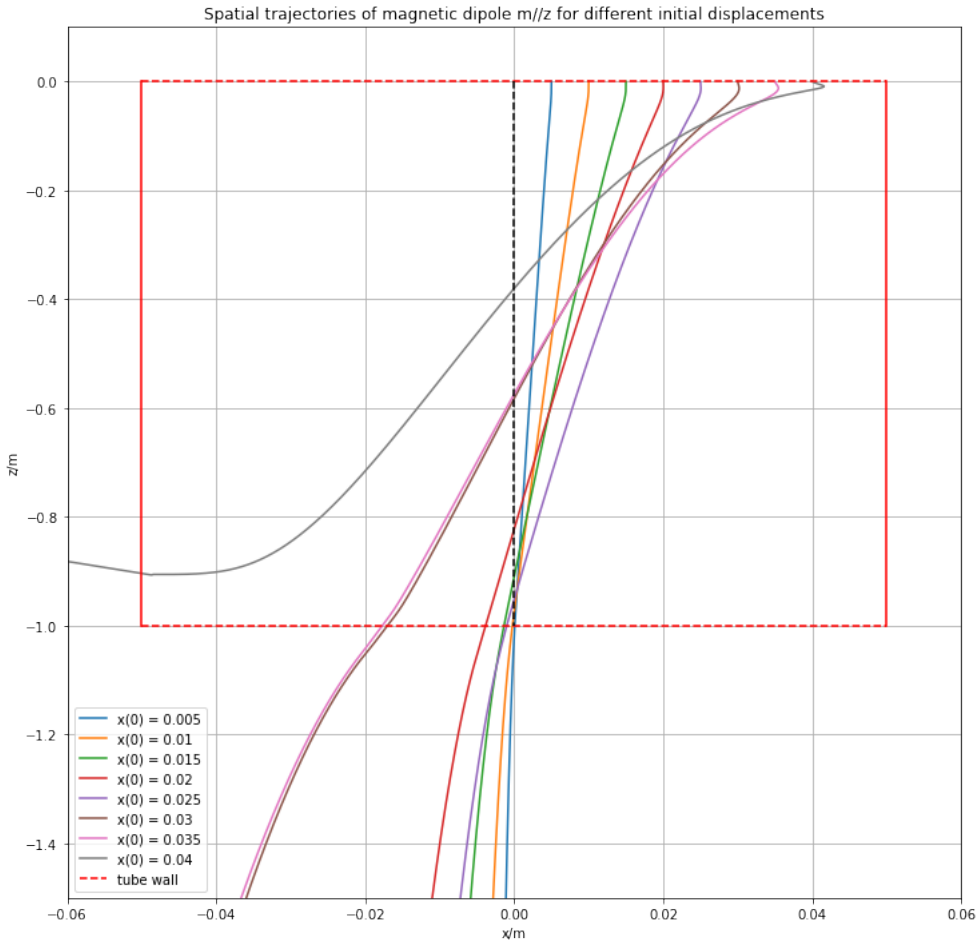

Figure 10: Plot of trajectories of magnets with different initial horizontal displacements, but released from rest in both directions. The grey curve depicts abnormal behaviour for a magnet having left the tube (there is no "rebound" in the simulation). The simulation produced nonsense results for this case, the magnet kept rising at high velocity after having escaped the tube laterally. This anomaly must be checked in future to see whether the correctness of the entire physical and computational model inside the tube is compatible with this strange behaviour beyond the (imaginary) tube walls.

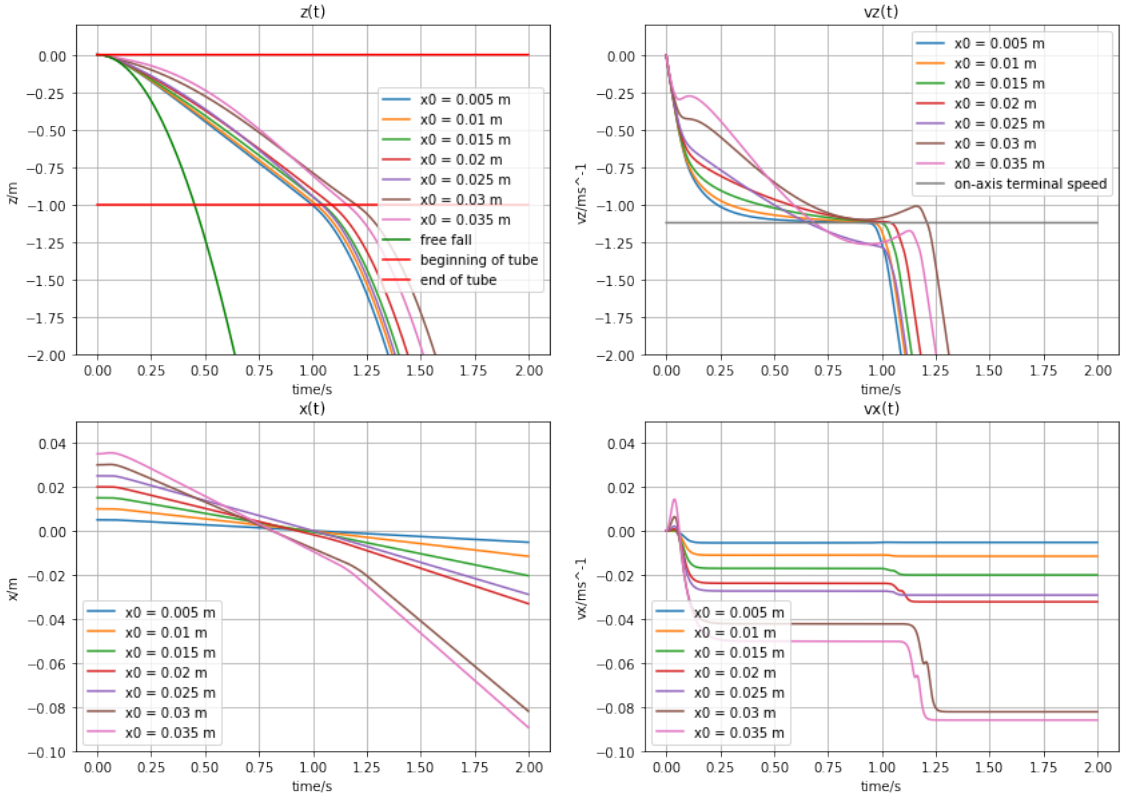

Figure 11: Coordinates and velocities for the same set of simulations for which trajectories are ploted above. Terminal speed for a centrally falling magnet in a long tube is 1.12 m/s for these physical parameters, so the top right graph is plausible in this respect. Also, after the eddy currents die out, all velocities assume the same gradient of $-g$. Note that in bottom right graph, magnet with smaller inital displacement of 2 cm is accelerated to higher lateral velocity than the one with 2.5 cm, thus breaking the consistency of the overall trend in velocities.

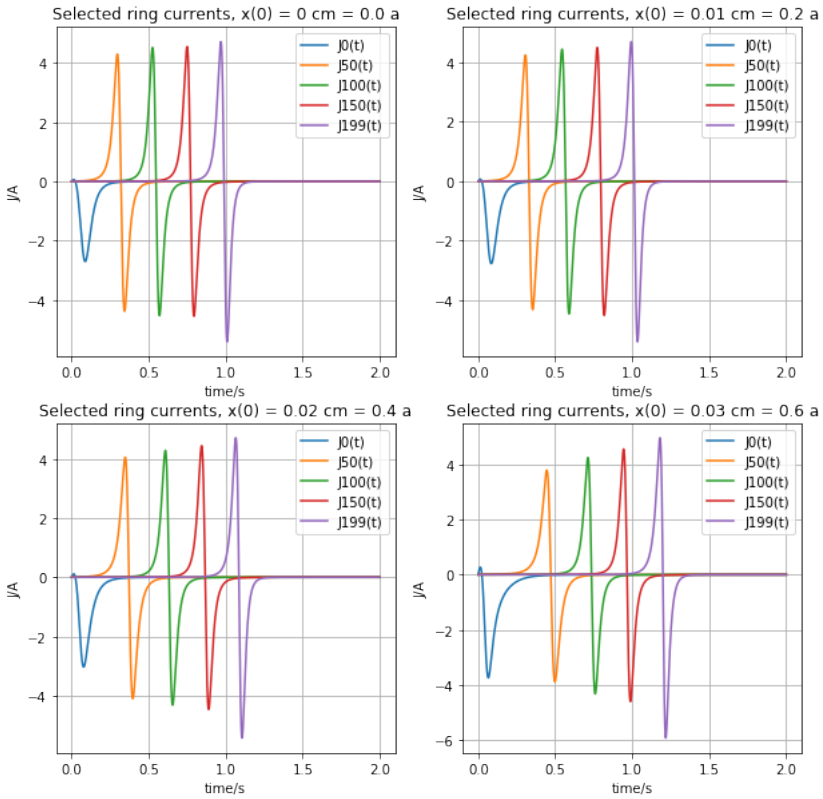

Figure 12: Currents in different ring elements along tube ($J_n(t)$ for $0 \leq n < N = 200$). As the magnet starts at the level of the upper edge of the tube, there is only one side of "Z"-shaped curve for first ring, at least for the centrally located magnet. Currents die out shortly after the magnet has left the tube.

3.3 Fall with rotation

Full analysis of simulation outcomes and their dependence on various parameters is not finalised and not inclueded here yet. The formulae for forces and voltages derived in subsection 2.3 are plotted here:

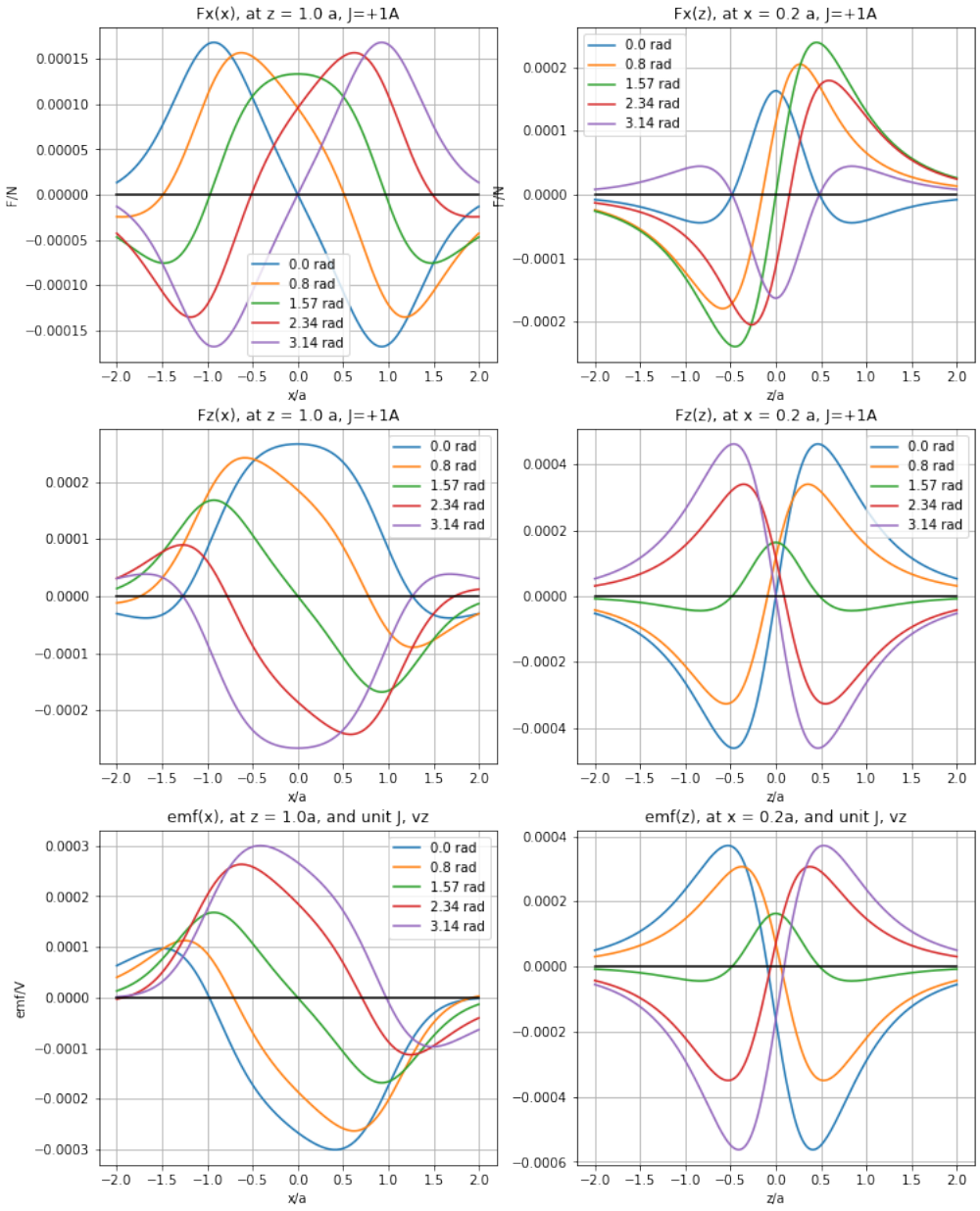

Figure 13: Forces in both directions and ϵ_{mag} ploted agains both axes for a range of tilt angles α. The absolute scale is decided by a choice of physical parameters and is not important in this example. NOTE the strange behaviour of graph of emf(x) - this needs further verification. (There is a need to check the graphs for the code, as well as the derivations, there is no reason for any assymetric shape for this curve for angles of 0 and π, this should be done in autumn 2020 prior to spending time on analysis of simulation outcomes)

4 Extension to superconductive case

This part of research has not been started yet, as a working classical (conducting) model was defined as a pre-requisite for working on superconductive tube.

5 Conclusion

The purpose of this work (disregarding the transition to superconducting case, which is left for future) was to establish a reliable numerical procedure for calculating the dynamics of magnet falling through a conducting tube. Expressions were derived for forces and induced voltages in the ring. However, the numerical implementation which would take into account the self-inductance of the tube is not working yet. The results of simulations are not yet reliably tested and should undergo a thorough review before continuing. This should start from checking all the algebra, up to the algorithmic implementation. The code for rotating magnet was tested very little. The main source of divergent or at least physically implausible behaviour seems to occur whenever magnet approaches the edges of tube. This may likely point to fundamental mistakes in underlying physical equations for forces. Alternatively, it might be artifact of our strange model, which treats the tube as non-material, and only interacting through (macroscopic) electromagnetic forces between magnet and induced currents. More work needs to be done to tell these apart and to analyze the behaviour of the rotating magnet.

References

1 G. Donoso, C. L. Ladera, and P. Martín, "Magnet fall inside a conductive pipe: Motion and the role of the pipe wall thickness," Eur. J. Phys. 30, 855–869 (2009)

2 G. Donoso, C. L. Ladera, and P. Martín, "Damped fall of magnets inside a conducting pipe" Am. J. Phys. 79, 193–200 (2009)

3 C. L. Ladera, G. Donoso, and P. Martín, "On-axis and off-axis fall and the role of the pipe wall thickness" Lat. Am. J. Phys. Educ. 6, 216-221 (2009)

4 Yan Levin, and Felipe B. Rizzato. "Superconducting pipes and levitating magnets." PHYSICAL REVIEW E 74, 066605, (2006).

5 Tim Welsh and Greg Severn, 2012 ALPha Conference on Laboratory Instruction Beyond the First Year of College, University of Pennsylvania and Drexel University, Wednesday, July 25 - Friday, July 27, 2012

6 D Williams et al 2019 Phys. Educ. 54 045019

Appendices

Simulation code and accessory files can be found at: `https://github.com/mokanik/magnet_summer_research_2020`
Analytical expressions for forces and induced currents can also be found there.